Computers and Chemical Engineering 97 (2017) 13–26

Contents lists available at ScienceDirect

Computers and Chemical Engineering

journal homepage: www.elsevier.com/locate/compchemeng

A comparison of the shrinking core model and the grain model for the iron ore pellet indurator simulation

Hyungjun Ahn, Sangmin Choi*

Department of Mechanical Engineering, Korea Advanced Institute of Science and Technology, 291 Daehak-ro, Yuseong-gu, Daejeon 34141, Republic of Korea

ARTICLE INFO

Article history:
Received 28 July 2016
Received in revised form 10 October 2016
Accepted 7 November 2016
Available online 11 November 2016

Keywords:
Iron ore pellet
Straight-grate indurator
Coke combustion
Shrinking core model
Grain model

ABSTRACT

The current study revisits the particle combustion modeling in the simulation of iron ore pellet indurator, which is the process to dry and fire the pellets as a pretreatment for blast furnace. Although the shrinking core model has been frequently used in the previous studies due to its simplicity, its limitation for the porous pellet should have been evaluated. Instead, the grain model could have been used as it conceptually gives the better description. In that context, the shrinking core model is compared against the grain model in the simplified isothermal condition and the complete indurator simulation to demonstrate the applicability. Despite the possible differences in the conversion profiles along the reaction regimes, the models provide apparently reasonable bed temperature results for the normal indurating conditions. However, the shrinking core model needs to be applied with caution and its validity should be questioned when the operating conditions change.

1. Introduction

Mathematical simulation for the industrial solid processes has widely been utilized because the direct performance measurement during the commercial operation would be difficult if not impossible. Industrial applications for solids processing are commonly associated with the gas-solid particle heterogeneous reactions. Representation of the complicated nature of the gas-solid reaction itself has long been an issue, and various types of particle reaction models have been proposed. Since the solid bed performance and productivity are largely affected by the gas-solid reactions, the proper reaction modeling is crucial in constructing a process simulation.

In a bed model, the reaction rate of a solid component is commonly described by applying a reaction model to the assumed representative particle. Since a reaction model is involved in the iterative bed calculation, a concise and analytical function for a global reaction rate would be preferred. A reaction model would be selected compromising a sophisticated description and a modeling efficiency. In doing so, appropriateness of the adopted reaction model should firstly be investigated regarding the particle characteristics in the reaction environment. However, bed simulations occasionally give an impression of modeling particle reactions with oversimplification, which may limit its validity over the range of operation conditions. In that context, the current study is specifically to reassess the single particle combustion models in the iron ore pellet indurator simulation.

As the feed of blast furnace, the typical iron ore pellet is made of mostly iron oxide mixed with coke, and limestone with water. Induration is basically to heat up the pellets for drying and thermal strengthening. Fig. 1 shows the schematic illustration of the straight-grate pellet indurator, which consists of the consecutive stages for up and down draft drying (UDD, DDD), preheating (PHZ), firing and after-firing (FZ, AFZ), and cooling (CZ1, CZ2) (Thurlby et al., 1979). Gas temperature and flow rates are controlled for each of the stages, and gases are partly recycled for energy efficiency. The bed temperature is considered to be the first priority in the process operation and modeling. The external gas supply plays the primary role in the bed temperature control, and coke in the pellet also provides the supplement heat. The typical coke content is as low as about 1 or 2 wt.-% of the pellet, but its combustion heat is around 30 MJ/kg, which almost controls the energy balance. On the other hand, water drying is arranged to be completed in the initial stages at relatively low temperature. The impact of endothermic limestone decomposition also seems less critical, considering its content and the heat of reaction. Other reactions, such as magnetite oxidation depending on the raw ore type, can be included but are not considered at this time.

Reaction modeling for a pellet needs to consider the particle characteristics as a porous spherical agglomerate of fine

* Corresponding author.
E-mail addresses: aj1983@kaist.ac.kr (H. Ahn), smchoi@kaist.ac.kr (S. Choi).

http://dx.doi.org/10.1016/j.compchemeng.2016.11.005
0098-1354/

Nomenclature

A	(Specific) particle surface area (m^2/m^3, m^2)
C	Concentration of the component ($kmol/m^3$)
C_p	Specific heat (kJ/kg K)
D	Diffusion coefficient (m^2/s)
d	Diameter (m)
F	Particle shape index for particle reaction models
f_g	Gas flowrate ($kg/m^2\ s^{-1}$)
f_s	Bulk density of solid (kg/m^3)
$g_F(X)$	Solid conversion function defined in the grain model
H	Enthalpy/heat of reaction (kJ/kg)
h	Convective heat transfer coefficient (kJ/m^2 s K)
K^e	Equilibrium constant
k	Thermal conductivity (kJ/m s K)
k_r	Rate constant (m/s)
k_m	Mass transfer coefficient (m/s)
L	Length (m)
M	Mass in the unit volume (kg/m^3)
N	Moles of the component
N_{Re}	Reynolds number $\left(=\rho uL/\mu\right)$
N_{Pr}	Prandtl number $\left(=C_p\mu/k\right)$
N_{Nu}	Nusselt number $\left(=hL/k\right)$
N_{Sc}	Schmidt number $\left(=\mu/\rho D\right)$
N_{Sh}	Sherwood number $\left(=k_mL/D\right)$
N^*_{Sh}	Modified Sherwood number in the grain model
P	Pressure (Pa)
$p_F(X)$	Solid conversion function defined in the grain model
R	Gas constant (kJ/kmol K)
R_i	Rate of reaction i (kg/m^3 s)
r	Radius of particle (m)
T	Temperature (K)
t	Time (s)
t^*	Dimensionless time in the grain model
u	Velocity (m/s)
V	Volume (m^3)
W	Molecular weight
X	Solid reactant conversion fraction
z	Coordinate in the bed height

Greek letters

α	the fraction of heat distribution in the reaction
ε	Porosity
μ	Viscosity (kg/m s)
ν	Stoichiometric coefficient of solid reactant which makes the coefficient of gaseous reactant unity
ρ	Density (kg/m^3)
σ	Dimensionless reaction modulus in the grain model
τ	Tortuosity

Subscripts

b	Bed
c	Coke
eff	Effective value
g	Gas phase / grain particle
l	Limestone
o	Initial (original) value
p	Particle / pellet
s	Solid phase / particle surface
w	Water

Superscripts

e	Equilibrium value
c	Critical value

component grains, as schematically illustrated in Fig. 2(a). The shrinking core model was widely used in the previous indurator simulations, which has helped to make the situation simple (Barati, 2008; Hamidi and Payab, 2003; Majumder et al., 2009; Sadrnezhaad et al., 2008; Tan et al., 2016; Wang et al., 2012). However, the background or the applicability of the model should have been discussed together with the modeling efficiency. The shrinking core model for a porous particle would become valid only when the reaction is controlled by inward diffusion where the reaction proceeds with the core-shell structure as the model depicts. Otherwise, the model would properly represent only a part of the reaction history (Do, 1982; Melchiori and Canu, 2014; Valipour and Saboohi, 2007; Wen, 1968; Wen and Wang, 1970). Moreover, the shrinking core model in the previous studies seems to have been used diversely with ambiguity or arbitrariness in the relevant parameters.

Nevertheless, the validity of a process simulation has been frequently shown simply by comparing the overall bed temperature profiles for the given process condition. However, considering the limitation and the simplification in the reaction modeling, the validity of the simulation may not be guaranteed when the operation conditions change. Meanwhile, the other reaction models, such as the grain model, could also have been used for more rigorous expression despite the increased complexities in the modeling. In this study, the application of the shrinking core model to coke combustion in the pellet is investigated by comparing against the grain model. The models in the analytical form are compared in the simplified condition, and the comprehensive simulation in the straight-grate indurator system is presented. By doing so, this study aims to demonstrate the possible limitations or the applicability of the shrinking core model.

2. Reaction models for pellet indurator performance simulation

2.1. Concepts of gas-solid reaction modeling

A generic reaction equation involving gaseous and solid reactants which generate gaseous and solid products can be written as Eq. (1). Assuming a globally complete combustion, coke combustion reaction can be written simply as Eq. (2) in which the stoichiometric coefficients are all unity.

$$aA(g) + bB(s) \rightleftarrows cC(g) + dD(s) \tag{1}$$

$$O_2(g) + C(s) \rightarrow CO_2(g) \tag{2}$$

Generally, the reaction between the gas and the solid particles is considered to be dependent on chemical reaction kinetics and diffusion of the gaseous matters. A thorough gas-solid reaction modeling would at least include fundamental equations of mass balances for single gaseous and solid species, concentrations of gaseous species and the solid reactants, total mass balances for the gas and the solid phases, molar flow or flux of single gaseous species and total gas phase, energy equation within a particle, as well as the equation of state, property estimations, effective diffusivity, effective thermal conductivity, heat and mass transfer coefficients, overall degree of conversion, reaction rate equation, and so forth (Patisson et al., 1998).

To reduce the complexities, the reaction modeling approaches used to adopt simplifying assumptions. The pseudo-steady-state approximation eliminates the transient term in the gas phase which makes the governing equations simple to produce the analytic solutions. Furthermore, the reaction is often assumed to be in the isothermal condition which also facilitates simplified analyses. Equimolar counter-diffusion is assumed when the stoichiometric coefficients of gaseous reactant and product are identical, so the effect of the net gaseous flux can be neglected. Of course, the limitations on the validity of those simplifications have occasionally been pointed out in the literature. For those cases, numerical solution procedure would be required to solve the whole set of equations, which is far more complicated than an analytical function or simpler explicit expressions (Patisson et al., 1998; Valipour and Saboohi, 2007; Wen and Wang, 1970). Nevertheless, the simpler analytical approach has also been shown to be useful due to the various criteria obtainable, and it is also favorable for the circumstances of bed reactors (Gómez-Barea and Ollero, 2006; Melchiori and Canu, 2014; Wen and Wang, 1970).

Various reaction models hitherto proposed can also be categorized by the manner of the reaction progression which each model illustrates. The heterogeneous type model assumes the structure of the unreacted core and the porous product shell divided by the narrow reaction interface which shrinks inward. This can be easily imagined for a nonporous particle which is initially impervious to the gaseous reactant. The core-shell structure can also be found when the relative degree of diffusion is far smaller than chemical reaction kinetics so the diffusion controls the reaction, i.e., the diffusive regime for the reaction. The shrinking core model is the most widely used one for the heterogeneous reaction. On the opposite side, the reaction may proceed uniformly throughout the particle with the constant concentration of gaseous reactant as homogeneous model depicts. This would occur when the particle is highly porous or the diffusion is a lot faster than reaction kinetics, that is the kinetic regime. In many practical situations, the reaction progression is likely to be in between the two extremes as represented by the intermediate type models including the grain model (Valipour and Saboohi, 2007; Wen, 1968). The reaction progression of the shrinking core model and the homogeneous model can be expressed by the grain model as its two special cases. The terms of the continuous model or the zone model also seem to include the intermediate manner of the reaction progression. The shrinking core model and the grain model in the form of the analytical function are as in the following sections.

2.2. Shrinking core model

Regardless of the reaction regimes, the model assumes the shrinking reaction interface in a nonporous particle leaving the porous product shell as in Fig. 2(b). In the figure, C_A is the concentration of the gaseous reactant A, as denoted in Eq. (1), along the radial direction in the particle which decreases from the bulk gas concentration at the particle surface to zero at the reaction interface. The shrinking core model for the reaction i can be written generally as in Eq. (3). The model describes the reaction progression with chemical reaction kinetics, particle film diffusion, and the effective diffusion through the outer porous product layer, as shown in the denominator. In the rate equation, parameters including the particle surface area A_p, the outer particle radius r_o, and the unreacted core radius r_c should be based on the same particle. The equilibrium gas concentration can be omitted when the reverse of a reaction is negligible. It has been generally suggested that the approximation using the model may practically be sufficient in many industrial applications (Ishida and Wen, 1971; Levenspiel, 1999; Melchiori and Canu, 2014; Wen, 1968)

$$R_i = \frac{\nu W_s A_p (C_g^e - C_g)}{\frac{r_o^2}{r_c^2 k_r} + \frac{1}{k_m} + \frac{r_o(r_o - r_c)}{D_{\text{eff}} r_c}} \tag{3}$$

$$D_{\text{eff}} = D_{AM}\varepsilon_p/\tau \quad \text{where} \quad \tau = \varepsilon_p^{-0.41} \tag{4}$$

The coke combustion rate in the pellet can be readily calculated using the shrinking core model as in the previous indurator models. The intrinsic chemical reaction constant may be selected from the literature. The mass transfer coefficient on the pellet surface k_m is determined simply by the Sherwood number and the molecular diffusivity of the binary gas mixture D_{AM}. For the effective diffusivity, Eq. (4) has been frequently shown with the shrinking core model in the previous studies which deals with diffusion in the pellet. Even though the equation does not explicitly state Knudsen diffusion or information about pore sizes, it has been used as a convenient and less rigorous way to approximate the effective diffusivity in the pellet. In fact, the equation seems to have originated from the previous works to derive the effective diffusivity from the molecular diffusivity (Currie, 1960). The equation and the exponent value seem to have chosen among the set of data by some of the researchers in the early years of mathematical modeling for ironmaking processes and have been used customarily for an iron ore pellet (Barati, 2008; Majumder et al., 2009; Wang et al., 2012; Yagi et al., 1967; Young, 1977).

Nevertheless, the application of the shrinking core model to coke in the pellet still needs to be questioned. Firstly, the shrinking core model has a limitation in the description of the reaction progression in a porous particle. The reaction progression in a porous pellet would be the core-shell structure or uniform as in Fig. 2(c) and (d) with the different profiles for the gaseous reactant concentration C_A throughout the particle. However, the shrinking core model would be acceptable only in the diffusion–controlled regime. To be classified as in the diffusive regime, the reaction on a pellet should be faster enough than the inward diffusion or the particle size needs to be large (Do, 1982; Ishida and Wen, 1971; Küçükada et al., 1994; Melchiori and Canu, 2014). The model may have limitations in kinetic and intermediate regimes or when the transition of the reaction regimes exists. However, applicable conditions for the shrinking core model have been rarely discussed for the pellet indurator modeling.

Secondly, determination of the modeling parameters becomes confusing due to the assumption and the particle structure. The relevant parameters in the shrinking core model, such as the surface area, particle radius, and the diffusion coefficients, are used for a single nonporous particle. However, when the solid reactant is a small fraction mixed in the pellet, it becomes uncertain what the characteristic particle should be for the model. The particle can be either the pellet or the grain, or it may be assumed arbitrarily. In this regard, the model may need the treatment to correlate the pellet and the coke grain, as the global particle and the reacting constituent. Otherwise, the model may not adequately describe the status of the reacting particle.

2.3. Grain model

Regarding the ambiguity with the shrinking core model as mentioned above, the grain model can be more advantageous than the shrinking core model conceptually. Firstly, the arbitrary assumption for the reacting particle is not necessary as the grain model depicts the structure of the pellet and the grains with idealization. The grain model assumes that the porous pellet consists of nonporous fine lumps of reactant solids on which the reaction actually takes place. Thus, the grain model can further specify the reaction progression as the combination of chemical reaction kinetics, mass transport at the pellet surface, diffusion through the pellet, and diffusion through the product layer of the grain. Secondly, the

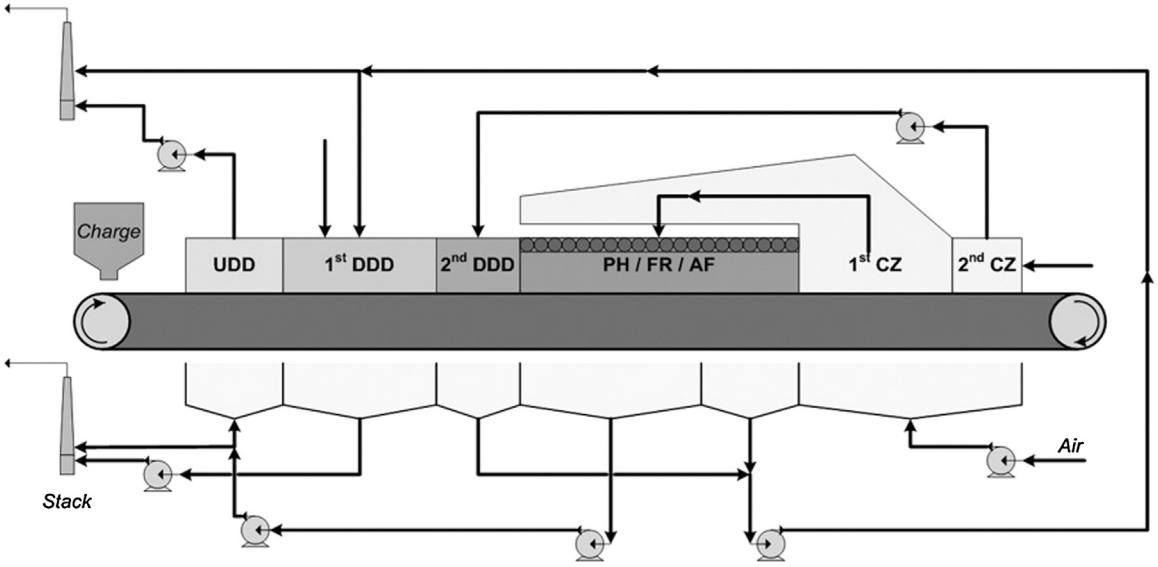

Fig. 1. Schematic diagram of conventional iron ore pellet induration process in straight-grate.

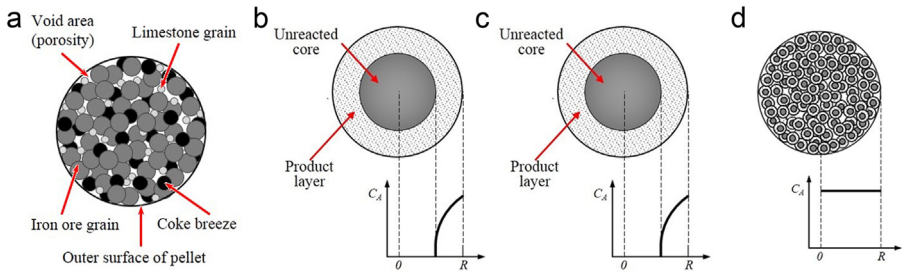

Fig. 2. Schematic illustrations for (a) an iron ore pellet considered in the current study (b) the shrinking core model (c) the grain model for diffusion controlled reaction (d) the grain model for chemical reaction controlled reaction with the variation of the concentration of the gaseous reactant C_A in the radial direction.

model can portray the reaction progression throughout the reaction regimes. While the reaction progression on the pellet varies as in Fig. 2(c) and (d) along the changing reaction regimes, the form of the rate equation or the parameters do not have to be modified or fitted. Essentially, the core-shell structure of the shrinking core model can be interpreted as a special case of the grain model.

In fact, the application of the grain model for a porous pellet and its validity can also be found in the previous studies. The original work of Szekely et al. is one of the most comprehensive descriptions of the grain model for a porous pellet. Based on the fact that the shrinking core model is applicable to the porous pellets only when the reaction is controlled by diffusion through a porous product layer, the authors emphasized that the importance and the advantage of the grain model is that it allows the interpretation of the reaction on a porous pellet under chemical or mixed controlled conditions, and enables the prediction of the overall reaction rates for various solid structures, such as different porosities and specific surface area. In the authors' work, the validity of the grain model for porous pellets was presented by introducing previous comparisons with experimental measurements, such as the reduction rate of nickel oxide by hydrogen and the reduction of hematite by hydrogen (Szekely et al., 1976). Among the recent works, Valipour and Saboohi considered the grain model in their mathematical model for the reduction of porous hematite pellets in a moving bed reactor which was validated to experimental data (Valipour and Saboohi, 2007). Nouri et al., applied the grain model to the simulation of the direct reduction reactor for porous hematite pellets by hydrogen and carbon monoxide. The prediction of their reactor simulation was compared with the experimental data from a commercial plant in terms of the outlet gas composition and final solid conversion. Although the separate validation of the reaction model in the single pellet scale was not presented, which is likely due to the limitations in the measurement from the operating plant, the good agreement of the final process parameters gives a glimpse to the appropriateness of the reaction model throughout the reactor process (Nouri et al., 2011). Melchiori and Canu presented the theoretical discussions to compare the simplified grain model and the shrinking core model throughout the reaction regimes. The authors concluded that caution is needed in the use of the kinetic constant for the shrinking core model as the model is erroneous out of the diffusive regime, which implies that the typical assumption that the shrinking core model is reasonable to any porous solids can be incorrect at some conditions (Melchiori and Canu, 2014). In short, the grain model is expected to enhance the validity of the reaction rate calculation for the wider range of induration conditions while increasing negligible computational load.

The rate equation of the grain model in the form of the explicit analytical function can be written as Eq. (5). The equation has been derived from the original set of the non-dimensional equations as explained in Appendix A.

$$R_i = -\frac{\nu W_s k_r C_g (1-\varepsilon_p)/r_{g,o}}{\frac{1}{3(1-X)^{2/3}} + \left(\frac{k_r r_{g,o}}{6D_g} + \frac{r_{p,o}^2(1-\varepsilon_p)k_r}{6D_{\text{eff}} r_{g,o}}\right)\left(\frac{2}{(1-X)^{1/3}} - 2\right) + \frac{k_r r_{p,o}^2(1-\varepsilon_p)}{3D_{AM} r_{g,o} N_{Sh}}} \quad (5)$$

In the equation, D_{AM} represents the molecular diffusivity on the pellet surface as explained above, and D_g is the diffusivity through the product solid layer of the grain. It has been said that the overall effective diffusivity through the porous solid matrix is governed not

only by molecular diffusion but also by the effect of Knudsen diffusion D_{AK} which is predominant in the micropores. The effective diffusion coefficient in the grain model is thus approximated using Eqs. (6) and (7) (Nouri et al., 2011; Szekely et al., 1976). The diffusivity in the developing product solid layer of the grain is assumed with Eq. (8) in which the value φ is set to 0.35. When the pellet is the mixture of multiple components, the pellet porosity ε_p should include the volume fraction occupied by inert components to the reaction, as well as the void area in the pellet.

$$\frac{1}{D_{\text{eff}}} = \frac{1}{\varepsilon_p^2}\left(\frac{1}{D_{AM}} + \frac{1}{D_{AK}}\right) \tag{6}$$

$$D_{AK} = \frac{4}{3}\left(\frac{8RT}{\pi W_A}\right)^{1/2} K_0, \quad K_0 = \left\{\frac{128}{9}\left[\frac{3(1-\varepsilon_p)}{4\pi r_g^3}\frac{\tau}{\varepsilon_p}\right] r_g^2\left(1+\frac{\pi}{8}\right)\right\}^{-1} \tag{7}$$

$$D_g = \varphi D_{\text{eff}} \tag{8}$$

3. Basic comparison of the reaction models

3.1. Simplification for the comparison

As a preliminary discussion, the two models are compared firstly in the hypothetical simple conditions prior to completing the entire indurator simulation. The calculation condition is simplified to the isothermal single pellet scale. In a bed simulation, the reaction rate of any point in the bed is determined with temperature, composition, properties, and other factors which changes by time in association with the neighboring area in the vertical and horizontal directions. However, as the calculation is simplified to a single pellet, the variables related to the bed become unnecessary. Moreover, temperatures of the gas and the solid are set to be identical, excluding the heat transfer resistance and the heat generation. Despite the unrealistic depiction, this simplification is adopted to restrict the temperature variation during the reaction history, so as to confine the differences in the overall reaction progression to the consequences of the different models at a certain reaction condition.

The pellet diameter is assumed to be 12 mm with sphericity of 0.95. The pellet porosity is set to 38% out of the slightly different values in the other studies and considered to be constant during the reaction. Although the actual grains constituting the pellet would have the size distribution and different shapes, the relevant descriptions have often been neglected in the indurator modeling. For convenience, the grains are assumed to be spherical with the mean diameter of 40 μm (Küçükada et al., 1994). Regarding the pellet composition, information tends to be limited to the specific components regarding the reactions, such as initial water content, limestone, and coke, in the previous indurator simulations. For convenience in this simplified comparison, the pellet is assumed to be comprised solely of 1.5 wt.-% of coke and ore. Iron oxides and other materials which constitutes the majority of the pellet needed to be approximated as hematite and inert components. The component grains are assumed to be distributed uniformly within a pellet. The gas composition is assumed as that of air. The rate constant $k_{r,c}$ for coke combustion is written as Eq. (9) in the Arrhenius equation form with A_r is 2.30 m/s K and E_r/R is 11,100 K (Hobbs et al., 1993). The well recognized Ranz-Marshall correlation in Eq. (10) is used for determining the mass transfer coefficient on the particle surface.

$$k_{r,c} = A_r T \exp\left(-E_r/RT\right) \tag{9}$$

$$N_{Sh} = 2.0 + 0.6 N_{Re}^{1/2} N_{Sc}^{1/3} \tag{10}$$

For the calculation of the models, temperature is increased from 400 °C to 1200 °C by 200 °C as the controlling variable. In each case, the models calculate the consumption of coke as combustion proceeds for the given temperature. Gas velocity could also be the variable for comparison as it may affect mass transport on the pellet. However, it needs to be noted that the impact of the gas velocities on the results was trivial in the range of 0.1–3.0 m/s, assuming the typical condition of the bed processes. The shrinking core model showed slightly faster progression when the gas velocity increased, but the differences were negligible compared to the changes by temperature.

3.2. The reaction rate equations

As the reactant gas condition and the reaction rate constant are used identically, the differences in the calculation results are attributed mostly to the assumption of each model which describe the reacting particle structure in relation to the diffusion effect. However, the shrinking core model in Eq. (3) can be interpreted in different ways due to the ambiguity as discussed above. Referring to the previous indurator modeling studies, several cases for the shrinking core model with modifications are prepared as a trial. The cases and the rate equations for comparison are as follow.

(a) GM — Grain model

The grain model is as described in Eq. (5) with diffusivity correlations in Eqs. (6)–(8).

(b) SCM1 — Basic form of the shrinking core model

In the previous indurator simulations, the rate equation of the shrinking core model was frequently presented in the basic form or occasionally described simply without the equations (Barati, 2008; Sadrnezhaad et al., 2008; Tan et al., 2016; Wang et al., 2012). Hence, the base case of the shrinking core model is considered as in Eq. (3) with respect to the pellet scale using the effectiveness diffusivity in Eq. (4).

(c) SCM2 — Shrinking core model with coke fraction

As mentioned above, the fraction of coke in the pellet may need to be considered as the actual reactant component. The model is also applied to the pellet scale, and the volume fraction of coke is multiplied to the SCM1 case as an arbitrary treatment as below.

$$R_c = -\frac{W_c A_p C_{O_2}}{\frac{r_o^2}{r_c^2 k_{r,c}} + \frac{1}{k_m} + \frac{r_o(r_o - r_c)}{D_{\text{eff}} r_c}} \times f_{v,c} \tag{11}$$

(d) SCM3 — Shrinking core model with modifying the effective diffusivity

The above shrinking core model cases used Eq. (4) for the effective diffusivity. As the approximation has been pointed out to be convenient but less rigorous approximation, the correlations in Eqs. (6)–(8) which were prepared to the grain model are tried based on the SCM2 case.

$$R_c = -\frac{W_c A_p C_{O_2}}{\frac{r_o^2}{r_c^2 k_{r,c}} + \frac{1}{k_m} + \frac{r_o(r_o - r_c)}{D_{\text{eff}} r_c}} \times f_{v,c}, \quad \frac{1}{D_{\text{eff}}} = \frac{1}{\varepsilon_p^2}\left(\frac{1}{D_{AM}} + \frac{1}{D_{AK}}\right) \tag{12}$$

(e) SCM4 — Shrinking core model with modifying the surface area

One of the previous indurator model presented the surface area A_p using the shrinking core radius r_c instead of the original pellet radius r_o (Hamidi and Payab, 2003). This is expected to make the overall rate diminish as the core radius would decrease along the reaction progression. However, there is no specific explanation for

this replacement and its physical validity neither, and thus it seems to be one good example of arbitrariness for the model.

$$R_c = -\frac{W_c A_p C_{O_2}}{\frac{r_o^2}{r_c^2 k_{r,c}} + \frac{1}{k_m} + \frac{r_o(r_o - r_c)}{D_{\text{eff}} r_c}} \times f_{v,c}, A_p = 4\pi r_c^2 \quad (13)$$

(f) SCM5 — Shrinking core model in the alternative form

The above shrinking core model cases are of the pellet scale explicitly as frequently presented in the literature. One of the previous study used the model in a different form as follows (Majumder et al., 2009). In this case, the correlation for the mass transfer coefficient seems to incorporate the film diffusivity and the effective diffusivity. Specifically, the mass transfer coefficient $k_{m,c}$ looks like the typical form of the film diffusion coefficient using Sherwood number, but the empirical diffusion coefficient of oxygen through coke is used instead of molecular diffusivity.

$$R_c = -\frac{6X_c \rho_s k_r X_{O_2}}{100 \rho_c d_c}, k_r = \left(\frac{1}{k_{r,c}} + \frac{1}{k_{m,c}}\right)^{-1} \quad (14)$$

$$k_{m,c} = D_{O_2-C} N_{sh}/d_{\text{eff}}, \qquad D_{O_2-C} = 0.435 \times 10^{-5} \left(T_g/298.15\right)^{1.5}/0.29^{-0.41}$$

3.3. Results

3.3.1. Overall conversion fraction profiles

Assuming that the approximation of the reaction progression from the grain model (GM) is realistic enough, the shrinking core model cases are compared as in Figs. 3 and 4 which show the coke conversion fraction profiles. The coke conversion fraction X is the ratio between the mass of consumed and initial coke component. It is considered simply as below in which $M_{c,o}$ and M_c are the mass of coke at the initial state and at certain times during the reaction.

$$X = (M_{c,o} - M_c)/M_{c,o} = 1 - M_c/M_{c,o} \quad (15)$$

Thus, the conversion fraction shows the degree of reaction progression from 0.0 for the initial state to 1.0 for the completion. Since the conversion fraction is a cumulative value, the relative degree of reaction rates can also be seen by the slope at any time. The reaction time is non-dimensionalized from 0.0 to 1.0 by dividing the elapsed time at any point to the entire reaction time which is identical to all the cases.

In Fig. 3, the conversion fraction profiles of the cases SCM1, SCM2, and SCM4 are plotted with the GM case. The SCM1 case gave typically overestimated unrealistic reaction rates. The entire reaction was completed in the middle of the reaction time even at the lowest temperature of 400 °C. Coke was depleted instantaneously in the higher temperatures so the plots were hardly noticeable as it lies vertically almost with the ordinate line. The SCM2 case had the similar order of the reaction rates to that of the GM case. However, this case showed large deviations as the progression was slower at low temperatures and faster at high temperatures. The results may support the assumption that the partial fraction of the solid reactant needs to be considered to the basic form of the shrinking core model but the further fitting of parameters are necessary to make the closer agreement. The SCM4 case had no difference to the SCM2 case at 400 °C, because the overall reaction rate is very low and the reaction was in the kinetic regime at this condition. As expected with replacing the outer pellet surface area with that of the shrinking core, using r_c instead of r_p in the numerator of the rate equation, the overall reaction progression of the SCM4 case was slightly lower than the SCM2 case. However, this case showed no significant advance from the SCM2 case.

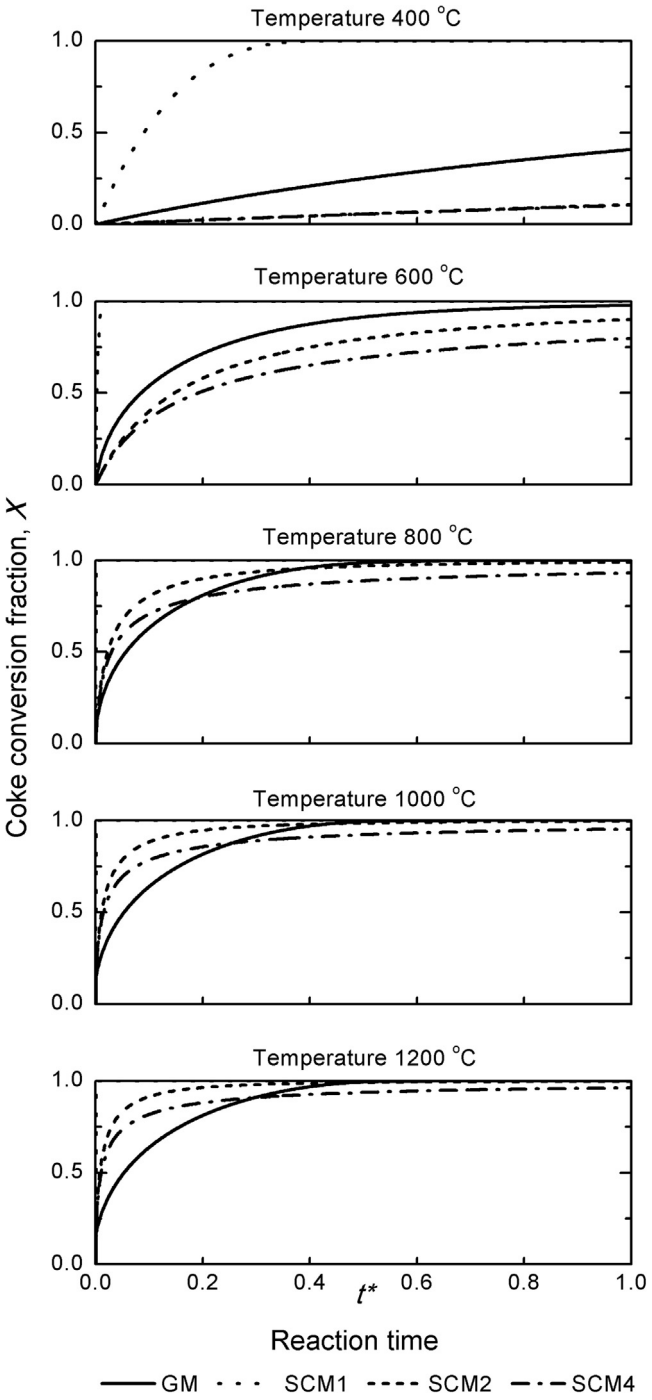

Fig. 3. The profiles of coke conversion fraction from GM (solid lime), SCM1 (dotted line), SCM2 (short dashed line), and SCM4 (dash-dot line) for different temperatures.

The conversion fraction profiles of SCM3 and SCM5 cases are compared with GM case in Fig. 4. The SCM3 case also seemed to have no difference to the SCM2 case at the lowest temperature as explained with the SCM4 case. The two cases became identical in this regime as the different effective diffusivity correlations had no effect while using the identical reaction rate constant. The differences between the two cases become evident with increasing temperature as the effect of inward diffusivity on the reaction increases. The SCM2 case tends to overestimate the reaction rate from the beginning and the degree becomes greater as temperature increases. This may be attributed to the limitation of the simple description of the inward diffusivity for the developing product

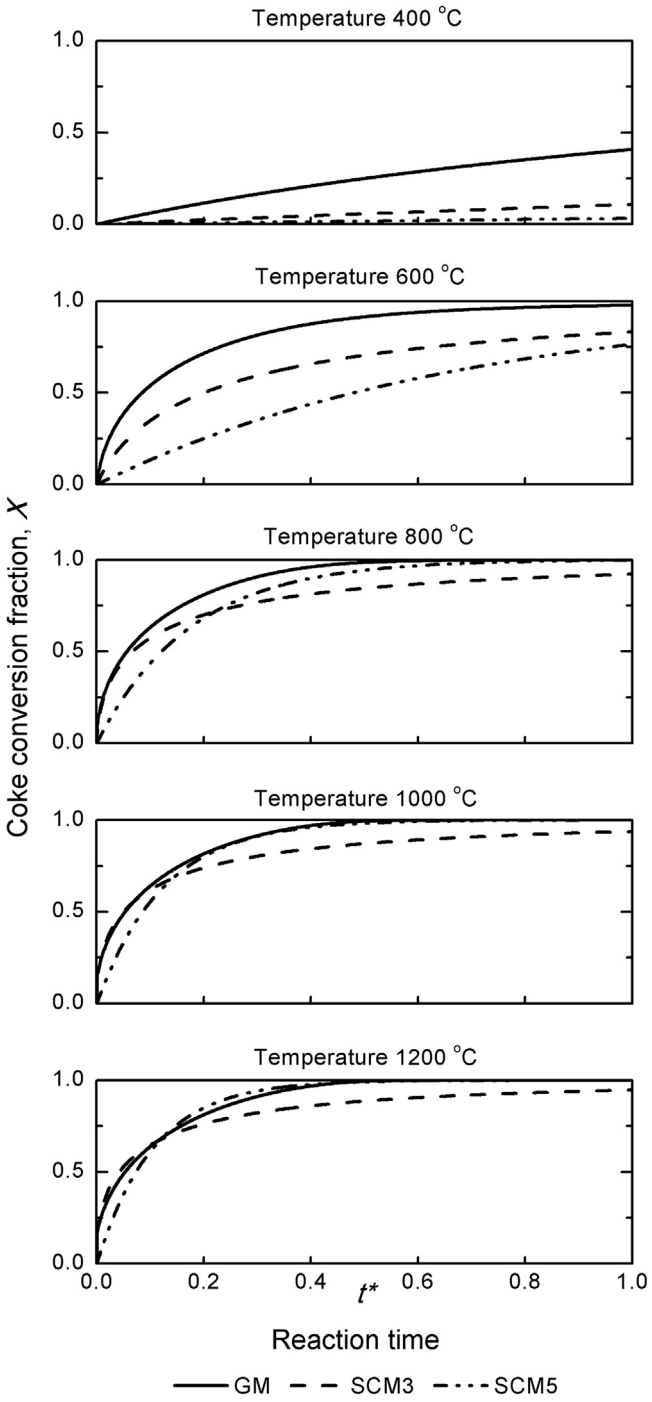

Fig. 4. The profiles of coke conversion fraction from GM (solid lime), SCM3 (dashed line), and SCM5 (dash-dot-dot line) for different temperatures.

shell used in that case. On the other hand, the SCM3 case that had replaced the correlation for the effective diffusion coefficient showed the closer agreement to the GM case. Nevertheless, the SCM3 case may still have limitations considering the deviations in lower temperatures and the slower completion in high temperature conditions. Compared to the other cases, the SCM5 case showed the closest results to the grain model except at the lower temperature conditions.

The reaction progression at different temperature conditions can also be seen with the reaction modulus σ^2, which is the non-dimensional parameter representing the relative importance of the chemical reaction kinetics and the diffusion on the reaction, thus a

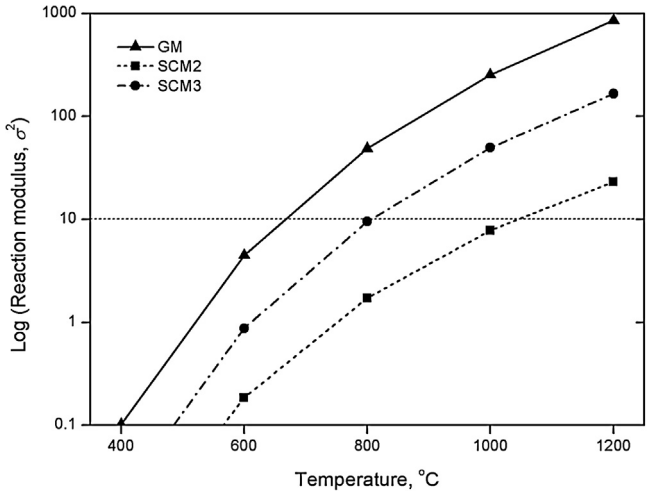

Fig. 5. The variation of the reaction modulus for the GM, SCM2, and SCM3 cases at different temperature in the log scale.

useful parameter to get a quick glimpse of the dominating reaction regime. According to the asymptotic analysis, the reaction is said to be chemical reaction controlled when the value is less than 0.1 and diffusion controlled when the value is above 10. The reaction modulus defined for the shrinking core system and the grain model can be written as below (Szekely et al., 1976). The shape factors for a grain F_g and a pellet F_p are given as 3 for sphere.

$$\sigma_{SCM}^2 = \left(\frac{k_r}{2D_{\text{eff}}}\right)\left(\frac{V_p}{A_p}\right)\left(1+\frac{1}{K^e}\right) = \frac{k_{r,c}r_p}{6D_{\text{eff}}} \tag{16}$$

$$\sigma_{GM}^2 = \left(\frac{V_p}{A_p}\right)^2 \frac{\left(1-\varepsilon_p\right)k_r F_p}{2D_{\text{eff}}}\frac{A_g}{F_g V_g}\left(1+\frac{1}{K^e}\right) = \frac{r_p^2\left(1-\varepsilon_p\right)k_{r,c}}{6D_{\text{eff}}r_g} \tag{17}$$

Fig. 5 shows the variation of the reaction modulus in the log scale for the GM, SCM2, and SCM3 cases at different temperatures. The horizontal short dashed line shows the asymptotic value of 10 above which is the diffusive regime. The reaction modulus generally increased with increasing reaction temperature, which implies that the degree of increase in the chemical reaction rate constant was relatively higher than that of the diffusion coefficient. According to the values of the GM case, the reaction was modeled almost in the kinetic regime at 400 °C and in the intermediate regime at 600 °C. Afterward, the reaction was in the diffusive regime from even below 800 °C. Given that the core-shell structure on a porous particle is valid when the reaction is diffusion-controlled, the larger share of the diffusive regime of the grain model may imply the more chances for the shrinking core model concept to produce the plausible results in the reaction environment. Consequences of using the different effective diffusivity in the SCM2 and SCM3 cases can also be seen from the figure. The effective diffusion coefficient in the SCM3 case would become smaller than that of the SCM2 case due to the consideration of Knudsen diffusivity. This led the SCM3 case to have the smaller reaction rate and the higher values of the shrinking core reaction modulus than the SCM2 case, which made differences in the reaction regime at the same temperature.

3.3.2. Diffusivity coefficients

Those variations in the overall conversion fraction profiles can be seen as the consequences by the different modeling concepts for the given pellet characteristics. Additionally, the effect of changing porosity to the reaction modeling may also be investigated. It

is generally expected that the overall reaction rate increases as temperature goes up with the given porosity and it is likely to diminish as porosity decreases at the given temperature. Moreover, the available reference data to compare are quite limited regarding the scope of the reaction progression in the iron ore pellet with the variation of pellet properties. Therefore, a simple observation of the overall conversion profile may be insufficient to discuss the effect of the modeling parameters. Instead, the differences in the reaction modeling are discussed with the variations of the diffusivity values for changing porosity at different temperature conditions. In the calculations, the pellet porosity is arbitrarily varied from the original value of 0.38 to 0.30, 0.20, and 0.10 while the interval of temperature from 400 °C to 1200 °C is maintained.

In the reaction modeling cases, the effective diffusivity is calculated using Eq. (4) in SCM1, SCM2, and SCM4 cases and Eq. (6) in GM and SCM3 cases. The molecular diffusivity D_{AM} for the film diffusion at the pellet surface was used identically in the two equations. The value was calculated using the Chapman-Enskog equation assuming nitrogen and oxygen as the two dominant component in the air. The value is dependent on temperature and the binary component, regardless of particle porosity. Therefore, the value of D_{AM} varies only with the temperature cases as seen in Fig. 6(a).

The calculation of Knudsen diffusivity D_{AK} in Eq. (7) is dependent on temperature, pellet porosity, grain size, and the gas component. Considering the equation for the given grain size and oxygen as the reactant gas component, the variation of D_{AK} can be displayed in terms of pellet porosity and temperature as in Fig. 6(b). It can be seen from the figure that the value generally increases along temperature increase at higher porosity, but the overall values are largely decreased roughly between 0.30 to 0.20. As a result, the relative magnitude of the Knudsen diffusion coefficient to the molecular diffusion coefficient D_{AK}/D_{AM} decreases as temperature increases and porosity decreases, as can be seen in Fig. 6(c). Since the effective diffusivity D_{eff} in Eq. (6) is expressed as the combination of D_{AM} and D_{AK}, the changes in the ratio of the two imply their relative contributions to the determination of the effective diffusion coefficient.

Fig. 7(a) shows the effective diffusion coefficient calculated from Eq. (6). The overall value deteriorated significantly as porosity decreases as low as 0.20, which is attributed to the decrease in the Knudsen diffusion coefficient as mentioned above. The drastic decrease in the effective diffusivity will result in the increase of the reaction modulus in Eq. (17) indicating the largely diffusion controlled situation, which may further lead to questions to what extent the particle can be considered as porous. As displayed in Fig. 7(b), the effective diffusion coefficient using Eq. (4) showed the larger values and more gradual variations than that from Eq. (6). It can be deduced from the results that the reaction progression modeled using Eq. (6) for the effective diffusivity will be much slower than other cases using Eq. (4) as pellet porosity decreases.

The differences in the order of the effective diffusion coefficients calculated from the two different equations can also be seen with the relative comparison to the molecular diffusion coefficient D_{eff}/D_{AM} as shown in Fig. 8. Specifically, rearranging Eq. (4) to make D_{eff}/D_{AM} on one side leaves the simple relation of $\varepsilon_p^{1.41}$ on the other side of the equation, which becomes the plot in Fig. 8(b). As mentioned above, the correlation and the exponent value seem to have originated from the experiment work to investigate the proper shape factor in the exponent of ε_p for different materials over various porosity (Currie, 1960). However, it needs to be noted that the value is correlated with the size of material which constitutes the porous media, as well as the specific porosity and the ratio

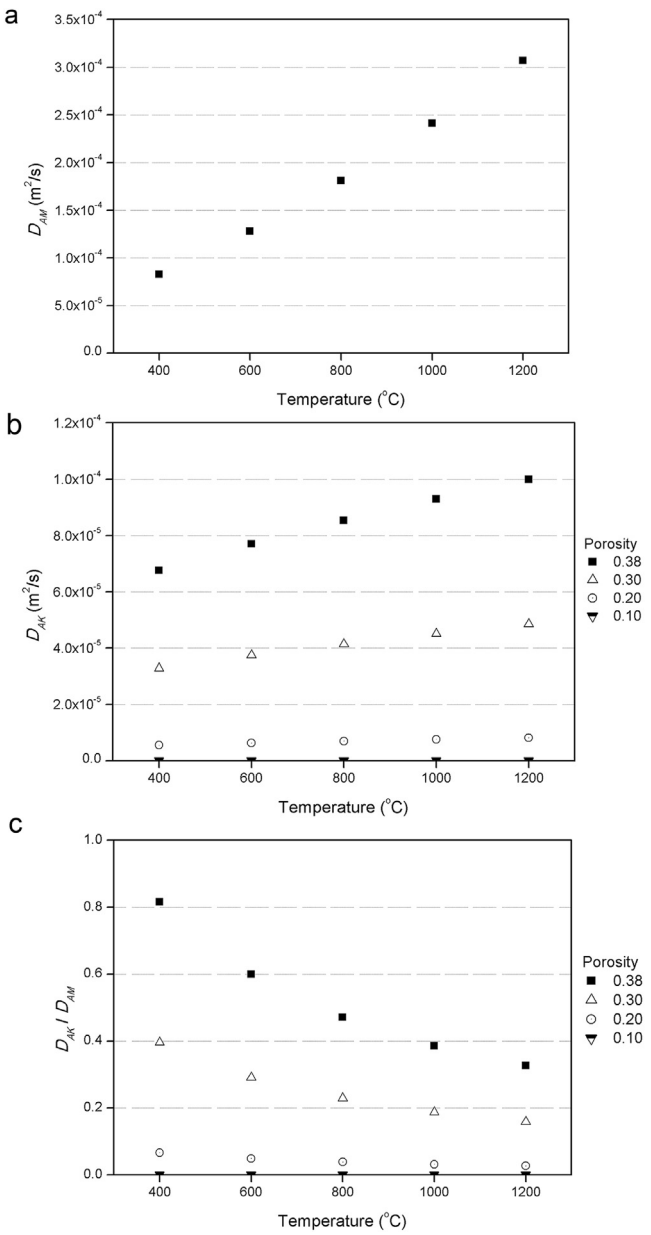

Fig. 6. The variation of diffusion coefficients at different temperature and porosity (a) the molecular diffusion coefficient (b) the Knudsen diffusion coefficient (c) the ratio between the Knudsen diffusion and the molecular diffusion coefficients.

of D_{eff}/D_{AM}. Therefore, it is doubtful whether the equation can be applied to the variety of the pellet conditions.

Despite the restricted calculation conditions, taking a glance at the differences in the overall reaction progression caused by simple modification in the rate equation is meaningful because it shows the consequences of arbitrariness in the use of the reaction models and the relevant parameter as the preliminary discussion. The results of the shrinking core model cases also imply that the model may need a fitting or treatment for the solid reactant which constitutes a fraction of the pellet. At the same time, the differences among the cases may not be critical in the overall indurator simulation as the condition of the external gas and the bed changes along the location and process time. Based on the discussions above, the cases of GM, SCM2, SCM3, and SCM5 are selected into the indurator simulation and compared in the following section.

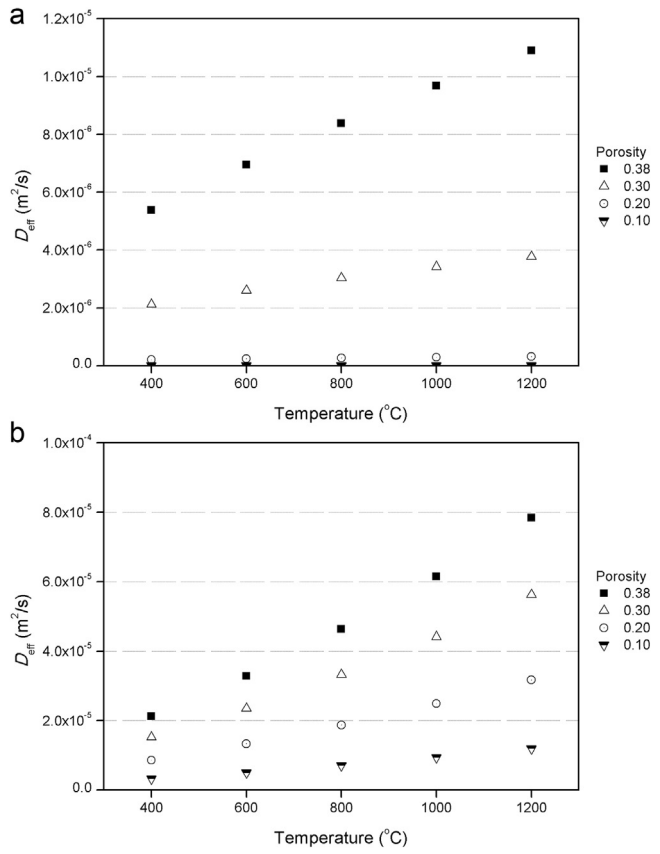

Fig. 7. The variation of the effective diffusion coefficients calculated from (a) Eq. (6) (b) Eq. (4).

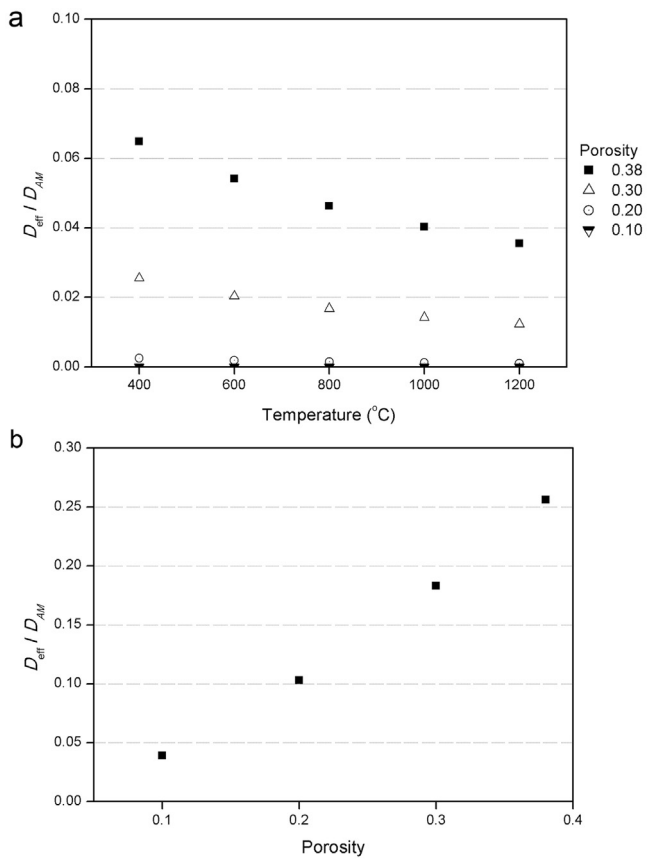

Fig. 8. The variation of the ratio between the effective diffusion coefficient and the molecular diffusion coefficient (a) the effective diffusivity from Eq. (6) (b) the effective diffusivity from Eq. (4).

4. Comparison for the indurator performance simulation

4.1. Straight-grate indurator model

As mentioned in the introduction, one of the typical approaches to calculate the reaction rate in the bed simulation is to assume a representative particle in each unit segment of the bed and apply a reaction model to the particle. Then, the reaction rate of the single particle is converted to that of the unit segment by considering the particle number density or other treatment. In the current indurator simulation, the reaction rate of a single pellet is firstly calculated using the grain model or the shrinking core model in one bed segment, and the change of mass and heat of reaction are determined from the calculated reaction rate on the basis of the unit volume of the bed segment. The calculation procedure continues throughout the entire bed area for the process time to obtain the overall bed temperature profile. Therefore, the definition of a reacting particle and its reaction modeling can be said to be critical to obtain the overall process parameters and determine the validity of the bed simulation. In the previous section, the reaction modeling has been discussed for a single pellet, and the current section describes the effects of the reaction models in the scope of the entire induration bed simulation.

Mathematical simulation of the straight-grate indurator typically consists of the bed simplification assumptions, governing equations, submodels to represent physico-chemical phenomena in the bed including heat and mass transfer and chemical reactions. Since the current study focuses on the particle reaction modeling as one of the submodels, the detailed descriptions for the overall process simulation including the simplifying assumptions and the governing equations are explained in Appendix B. It needs to be noted that the bed temperature profile has been presented as the most important result parameter in the previous studies for indurator modeling. This is mostly attributed to the limitations in the direct evaluation of process performance, such as fired pellet strength and bed productivity, from the mathematical simulation, and the bed temperature history is applied as an indirect measure to predict the process performance. As a result, most of the previous modeling studies aimed to produce bed temperature profiles while providing little information at the pellet scale.

Regarding the scope of the current study to compare the reaction models in the indurator simulation, the limitations in utilizing the process conditions and the results in the literature should also be noted. Most of all, a set of essential input process parameters should be accessible from one modeling study to conduct the entire indurator simulation and compare the results, but relevant information is usually provided insufficiently. Moreover, the results from the previous studies that had applied the shrinking core model to coke combustion were excluded as it is what the current study discusses about. Consequently, the available data for the separate validation of the grain model in the indurator condition was quite limited.

As an alternative, the indurator simulation for the reaction modeling cases is conducted in two steps. Firstly, the indurator model is validated to the condition without coke combustion as in Table 1 (Majumder et al., 2009; Thurlby et al., 1979). Fig. 9 is the simulated bed temperature profiles at four different levels of 5, 17, 29, and 41 cm from the bed top. In the figures, the solid line represents the results of the current simulation while solid square is the data excerpted from the reference (Thurlby et al., 1979). For reference, inlet gas temperature is plotted together in Fig. 9(a), the highest observation point in the bed. There were small deviations

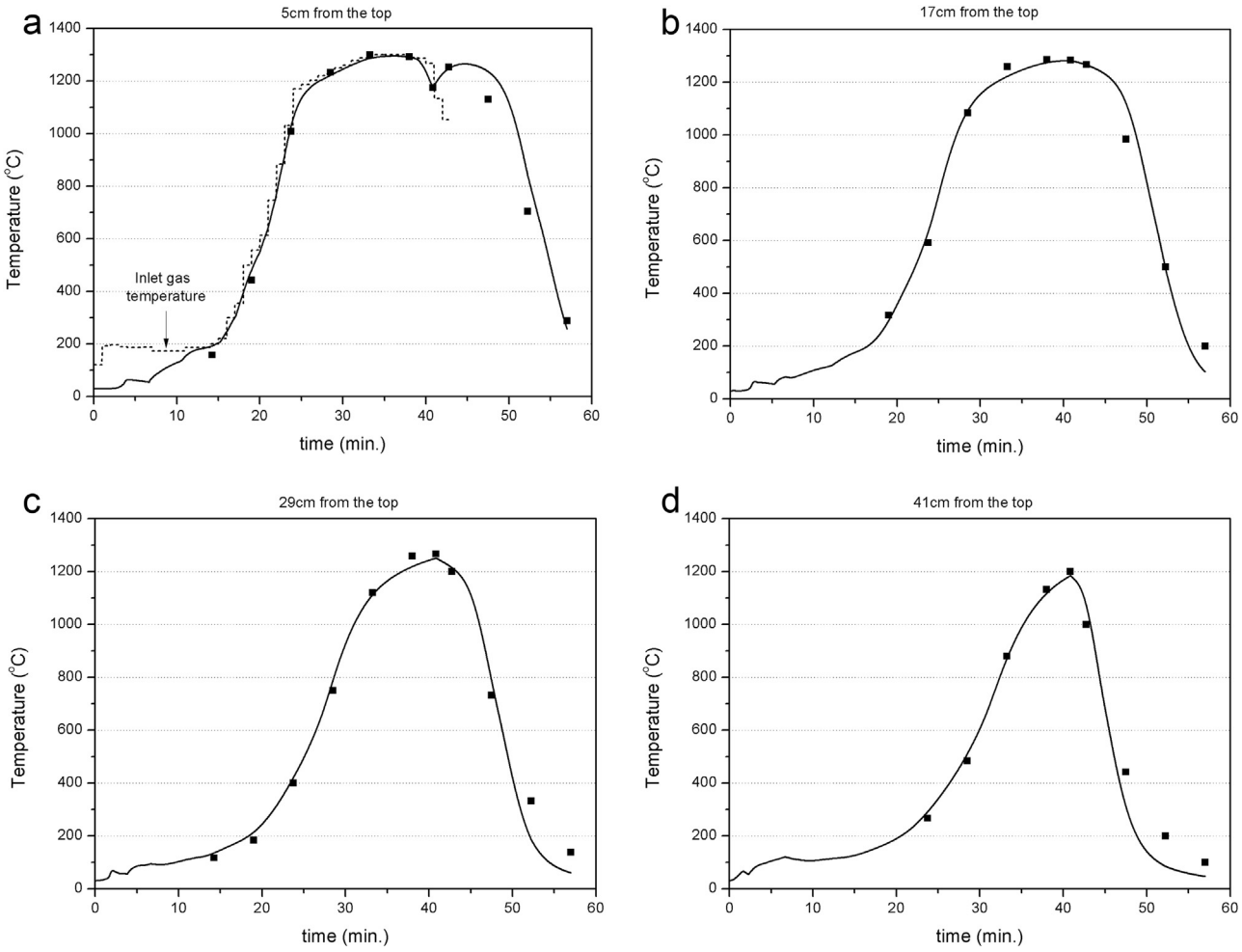

Fig. 9. Bed temperature profiles at different levels (a) 5 cm (b) 17 cm (c) 29 cm (d) 41 cm from the bed top. (■ experimental data from the reference,—the current simulation data).

Table 1
Simulation conditions for induration process.

Parameter	Value
Bed conditions	
Bed length (m)	120
Bed height (m)	0.55
Hearth layer height (m)	0.10
Grate area (m^2)	400
Grate speed (m/min.)	2.1
Bed porosity	0.4
Pellet conditions	
Pellet diameter (mm)	12
Grain mean diameter (μm)	40
Pellet sphericity	0.95
Pellet initial porosity	0.38
Initial moisture content (wt.-%)	10.0
Stage process time (min.) / Pressure drop (mbar)	
UDD	6.7 / 45
DDD 1st	10.5 / 40
DDD 2nd	4.8 / 40
PH, FR, AF	19.0 / 45
CZ 1st	11.4 / 50
CZ 2nd	4.8 / 35

at the cooling zone, but the bed simulation could well represent the variation of bed temperature as can be seen from the figures.

Then, based on the established indurator model, the simulations including coke combustion modeling are carried out for the selected reaction model cases, i.e., GM, SCM2, SCM3, and SCM5. For coke combustion, a pellet is considered to have 1.5 wt.-% of coke, as considered in the previous section, while maintaining the rest of the process conditions. Since the parameters in Table 1 is from the complete induration process without solid fuel, the addition of coke is a hypothetical modification to the existing process condition. This may not provide the direct validation of the grain model for coke combustion in the indurator simulation. Nevertheless, the comparison of the cases can be made on the same basis of the process simulation, which is still expected to be helpful to discuss the influence of the different reaction modeling cases.

4.2. Results

Fig. 10 is the bed temperature profiles with the different coke combustion modeling cases. Compared to Fig. 9, the longer duration of high temperature region could be observed especially at the lower part of the bed due to the addition of coke combustion. Overall, the different rate equations had small differences in the bed temperature except for the SCM5 case. The difference between the SCM5 case and the others were greater at the lower part of the bed. From the bed temperature results, it could be expected that the SCM5 case generated the slower reaction progression roughly in the preheating and firing stages. The reaction progression of the cases can further be seen with the coke conversion fraction profiles as in Fig. 11. The reaction in the SCM2 and SCM3 cases commenced at the similar time to the GM case as bed temperature began to

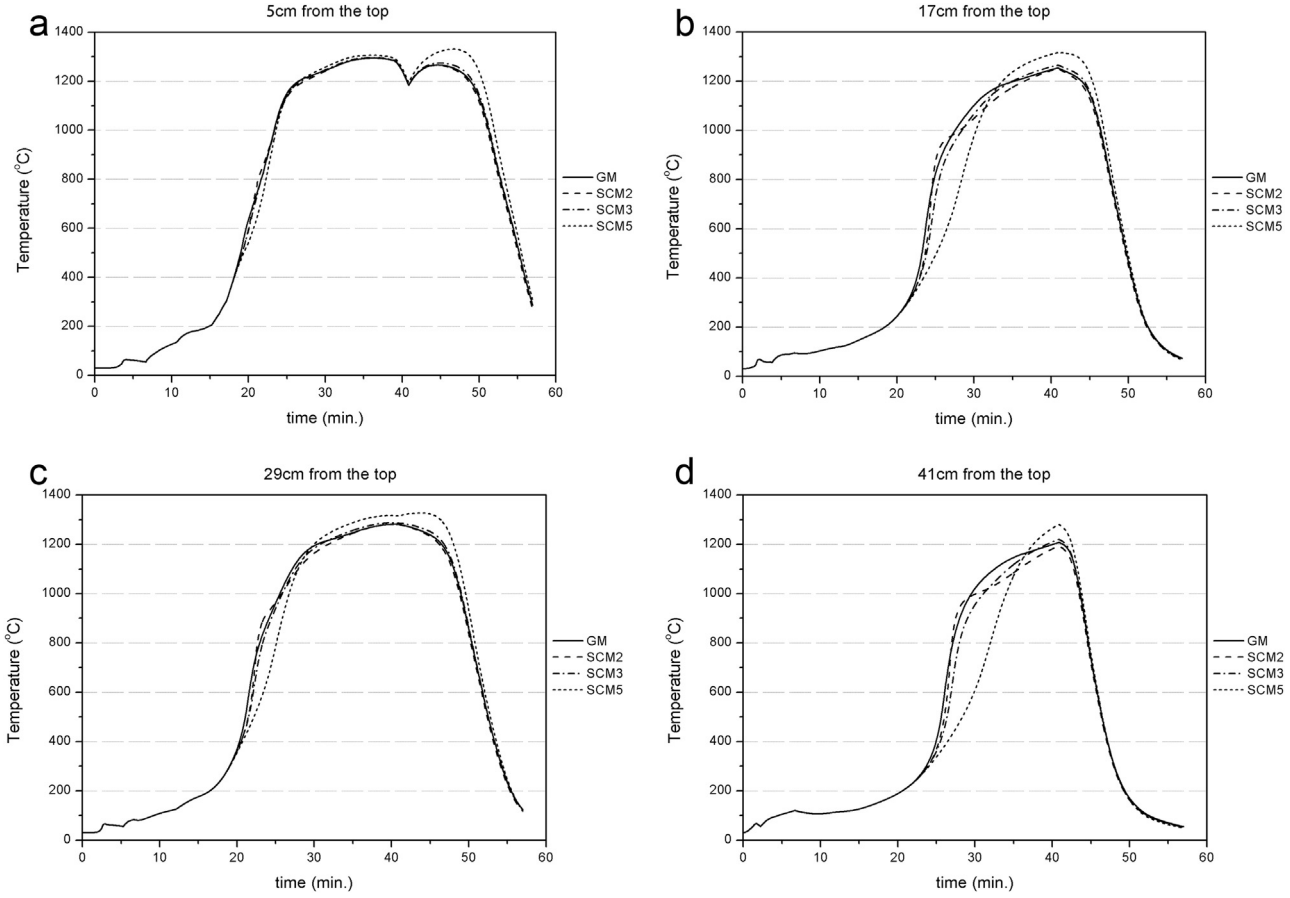

Fig. 10. Temperature profiles at the different bed levels for the cases of the particle reaction models.

increase in the preheating zone. Similar to Figs. 3 and 4, the SCM2 case showed faster progression than the GM case and the SCM3 case had slower progression. However, the SCM5 case showed the slower start in any level of the bed, and the reaction progression lagged behind the others so the reaction had not even completed during the process.

The conversion fraction profile at each level of the bed is accompanied by the variation of the reaction regimes using the grain model reaction modulus in Eq. (17). Each patterned area represents the kinetic regime ($\sigma^2 < 0.1$), the intermediate regime ($0.1 < \sigma^2 < 10$), and the diffusive regime ($10 < \sigma^2$), respectively. The shaded areas cover where the reaction takes place during the entire process. The figures firstly show that the reaction within the pellet would experience the changes in the rate controlling mechanism during the induration process. As can be seen from the figure, the grain model described the reaction which started in the kinetic regime then varied to the intermediate and the diffusive regimes as bed temperature increases.

It can be derived from the figures that the majority of the reaction progression occurred in the diffusive regime. The kinetic and the intermediate regimes also take the half roughly, but they seem less influential considering the relatively negligible reaction rate at the lower temperature zones. As mentioned previously, the porous pellet would have the core-shell structure in the diffusive regime as the shrinking core system portrays. The figure may imply that the longer duration of the diffusive regime in the grain model alleviated the conceptual differences between the grain model and the shrinking core model for the porous pellet and in the induration condition. Perhaps this was one of the background of using the shrinking core model in the previous indurator simulations presenting the plausible bed temperature results.

5. Conclusion

Mathematical simulation has widely been conducted for iron ore pellet indurator to understand the internal thermal state and to predict the performance. Simulations for the straight-grate system generally aims to obtain the bed temperature profiles incorporating the heat transfer and the reactions on the pellet. In constructing the bed simulation, the shrinking core model was preferred for the convenience of bed temperature calculations as it gives the simple and analytical function of the reaction rate. However, the model has the inherent limitations as a result of the assumption of the core-shell structure in the single species nonporous particle. Hence, the model might have needed caution when it is used for the coke in the pellet, as the small fraction of reactant in the porous agglomerate, which has not been focused sufficiently in the previous studies.

Comparison of the shrinking core model with the grain model implies that the shrinking core model might have needed a fitting to make the more realistic approximation. Preparing the different rate equation cases for the shrinking core model itself showed the arbitrariness in using the model for coke fraction in the pellet. Despite the possible differences, some of the shrinking core model cases showed the similar bed temperature profiles to the grain model case in the complete model of the conventional indurator condition. The similarity may be largely due to the low coke content and the dominance of the hot gas in the heat transfer to the bed. Moreover, it may also be attributed to the longer duration of the diffusive regime for the reaction, in which the core-shell structure becomes valid as the shrinking core model assumes. Those may explain the plausible temperature results in the previous indurator models using the shrinking core model.

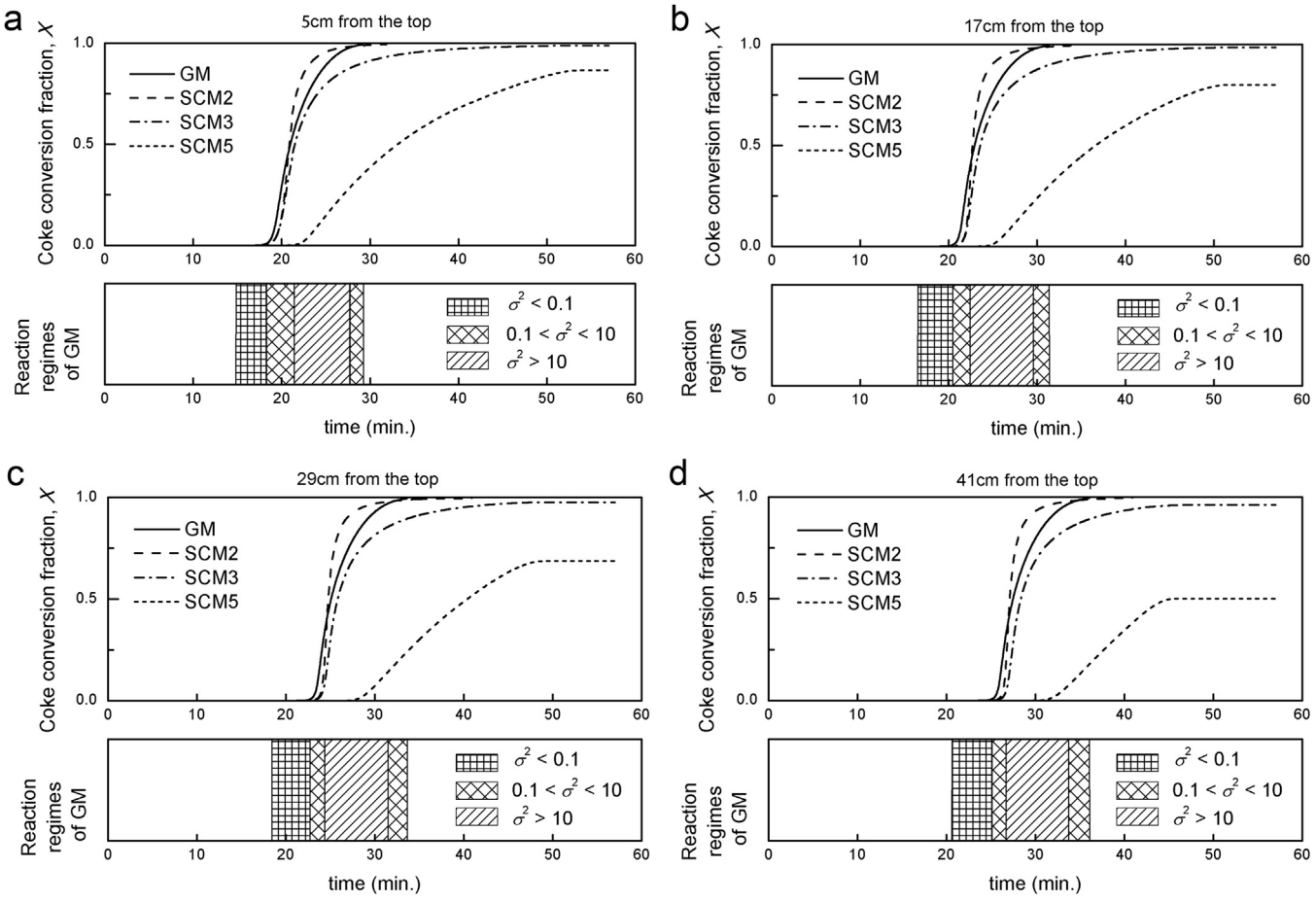

Fig. 11. The coke conversion fraction profiles for the cases of the particle reaction models.

Nevertheless, the similar bed temperature results for the given indurator condition may still not guarantee the validity of the shrinking core model when the operation condition changes. The comparisons of the conversion fraction profiles imply the possible discrepancies or errors in the detailed description of the reaction progression using the shrinking core model. The existing process may be changed for purposes, such as increasing solid fuel content, changing external gas temperature or composition, modifying the process configuration for optimization, and so forth. In those cases, inaccuracies from the reaction modeling can have the greater influence on the bed temperature and the process prediction. Therefore, the grain model would be more advantageous for further improvement and extension of the indurator simulation, because it can give more accurate and specific information for the pellet reaction as an advanced approach.

Appendix A. . The general dimensionless equations of the grain model

The analytical form of the grain model rate equation can be derived from Eq. (A1) together with the equations from Eqs. (A2)–(A7) in the non-dimensional form as originally presented. The shapes of grains and pellets are assumed to be spherical, so the shape factors for grain F_g and pellet F_p are given as 3 in the equations (Szekely et al., 1976).

$$t^* = g_{F_g}(X) + \sigma_g^2 p_{F_g}(X) + \sigma_p^2 \left[p_{F_p}(X) + \left(2X/N_{Sh}^* \right) \right] \tag{A1}$$

$$t^* = \frac{\nu k_r}{\rho_s} \frac{A_g}{F_g V_g} \left(C_{As} - \frac{C_{Cs}}{K^e} \right) t = \frac{\nu k_r C_{O_2}}{\rho_s r_{g,o}} t \tag{A2}$$

$$g_{F_g}(X) = 1 - (1-X)^{1/3} \tag{A3}$$

$$p_{F_g}(X) = 1 - 3(1-X)^{2/3} + 2(1-X) \tag{A4}$$

$$\sigma_g^2 = \left(\frac{k_r}{2D_g} \right) \left(\frac{V_g}{A_g} \right) \left(1 + \frac{1}{K^e} \right) = \frac{k_r r_{g,o}}{6D_g} \tag{A5}$$

$$\sigma_p^2 = \left(\frac{V_p}{A_p} \right)^2 \frac{\left(1-\varepsilon_p\right) k_r F_p}{2D_{\text{eff}}} \frac{A_g}{F_g V_g} \left(1 + \frac{1}{K^e} \right) = \frac{r_{p,o}^2 \left(1-\varepsilon_p\right) k_r}{6D_{\text{eff}} r_{g,o}} \tag{A6}$$

$$N_{Sh}^* = N_{Sh} \left(D_m / D_{\text{eff}} \right) \tag{A7}$$

In the right hand side of Eq. (A1), the first term is about the chemical reaction on the grains, the second term is about diffusion on the grains, and the two terms in the bracket represent the pore diffusion and the film diffusion on the pellet, respectively. The conversion functions $g_{F_g}(X)$ and $p_{F_g}(X)$ depend on the particle shape which are for a sphere currently. Substituting parameters from Eqs. (A2)–(A7) in Eq. (A1), differentiating the solid conversion fraction X with respect to t, and rearranging the equation give the rate expression as in Eq. (5) (Nouri et al., 2011).

Appendix B. . Governing equations of the straight-grate indurator model

For the convenience in the bed simulation, the packed particles are considered as the continuum of the two phases of the gas and the solid, which is the porous media approximation. The following

assumptions are adopted for the indurator simulation: (1) Pellets have identical size and composition and are uniformly distributed in the bed, (2) Pellets are assumed to be isothermal, (3) Uniform distribution of the ideal gas without channeling in the bed, (4) Gas flow in the vertical direction is dominant, thus one-dimensional gas flow is assumed, (5) Property variation is significant in the vertical direction, while widthwise and lengthwise variations are negligible, (6) Heat loss through bed walls is neglected, (7) Indurator process is in the steady state.

Those assumptions enable the bed to be simplified to the unsteady one-dimensional condition which is discretized vertically in the direction of gas flow. One column, a stack of unit segments in the vertical direction, corresponds to the domain for one time step in the unsteady one-dimension calculation. As the grate speed is assumed to be uniform, the time step in the unsteady one-dimension calculations can be matched to the bed length. Accordingly, the parameter results for the entire bed can be presented by consecutive display of the one-dimensional columns.

Governing equations consist of energy, mass, and species equations for the gas and the solid phases, the local momentum equation for the gas, and the equation of state. The energy equations include the effects of convective heat transfer between the gas and the solid, conduction within the solid phase, and the heat of reactions. The energy equation for the gas phase can be written as

$$\frac{\partial\left(f_g C_{p,g} T_g\right)}{\partial z} = \frac{\partial}{\partial z}\left(\varepsilon_b k_g \frac{\partial T_g}{\partial z}\right) - hA_s\left(T_g - T_s\right) + \sum_g (1-\alpha_i) R_i \Delta H_i \tag{B1}$$

and the energy equation for the solid phase is as follows:

$$\frac{\partial\left(f_s C_{p,s} T_s\right)}{\partial t} = \frac{\partial}{\partial z}\left[(1-\varepsilon_b) k_s \frac{\partial T_s}{\partial z}\right] + hA_s\left(T_g - T_s\right) + \sum_s \alpha_i R_i \Delta H_i \tag{B2}$$

In the equations, the distribution factor for reaction heat α is set to 0.5 for moisture condensation and 1.0 for the other reactions (Barati, 2008). The heat transfer coefficients for the pellet layer and the grate bar are determined using the following correlations, respectively (Barati, 2008; Küçükada et al., 1994; Thurlby et al., 1979).

$$N_{Nu} = 2.0 + 1.1 N_{Re}^{0.6} N_{Pr}^{1/3} \tag{B3}$$

$$N_{Nu} = 5.0 N_{Re}^{1/2} \tag{B4}$$

Material components considered in the present study are Fe_2O_3, Fe_3O_4, FeO, Fe, coke, $CaCO_3$, CaO, inert, and H_2O for the solid phase and N_2, O_2, CO, CO_2, H_2, H_2O for the gas phase. The mass balance equations for the gas phase and the solid phase are as follows:

$$\frac{\partial f_g}{\partial z} = \sum_g \Delta R_i \tag{B5}$$

$$\frac{\partial f_s}{\partial t} = \sum_s \Delta R_i \tag{B6}$$

and material component balance in the two phases are as follows:

$$\frac{\partial\left(f_g M_{g,k}\right)}{\partial z} = \sum_g \Delta R_{i,k} \tag{B7}$$

$$\frac{\partial\left(f_s M_{s,k}\right)}{\partial t} = \sum_s \Delta R_{i,k} \tag{B8}$$

For the local momentum equation for gas phase, the Ergun equation has been applied extensively to estimate the gas flow rate in the relation of pressure drop for the packed bed structure (Barati, 2008; Hamidi and Payab, 2003; Küçükada et al., 1994; Majumder et al., 2009; Sadrnezhaad et al., 2008; Thurlby et al., 1979). The gas velocity through the bed is determined at each stage by the given values of pressure drop.

$$\frac{\Delta P}{L} = 150\frac{\mu_g (1-\varepsilon_b)^2}{d_p^2 \varepsilon_b^3} u_g + 1.75\frac{\rho_g (1-\varepsilon_b)}{d_p \varepsilon_b^3} u_g^2 \tag{B9}$$

The equation of state is written as follows:

$$\rho_g = \frac{P_{atm}}{R_u T_g \sum\left(X_i / W_i\right)} \tag{B10}$$

Pellet water drying is also included in the indurator simulation. Drying is assumed to take place in two stages depending on the pellet water content and the critical content. Initially, water dries out at the pellet surface due to the difference in water content of the gas at the surface and its equilibrium concentration. As the pellet water content drops below the critical value, the dried shell is formed leaving the wet core until drying completes. The similar drying models can frequently be found in the literature, and thus not explicitly included for conciseness in this description (Barati, 2008; Hamidi and Payab, 2003; Küçükada et al., 1994; Majumder et al., 2009; Sadrnezhaad et al., 2008; Thurlby et al., 1979). Bed porosity may be given simply as the initial value referring to the literature or it can be approximated using the correlation relating size, density, sphericity of particles, and particle packing. Moreover, some of the studies introduced the physical deformation such as pellet shrinkage or changes in the bed height during induration (Barati, 2008). However, the degree of pellet shrinkage or the changes in the bed height and porosity are thought to have minor effects, and they are assumed to be constant to narrow down the current focus to the particle reaction modeling.

References

Barati, M., 2008. Dynamic simulation of pellet induration process in straight-grate system. Int. J. Miner. Process. 89, 30–39.

Currie, J.A., 1960. Gaseous diffusion in porous media. Part 2.—Dry granular materials. Br. J. Appl. Phys. 11, 318–324.

Do, D.D., 1982. On the validity of the shrinking core model in noncatalytic gas solid reaction. Chem. Eng. Sci. 37, 1477–1481.

Gómez-Barea, A., Ollero, P., 2006. An approximate method for solving gas-solid non-catalytic reactions. Chem. Eng. Sci. 61, 3725–3735.

Hamidi, A.A., Payab, H., 2003. Mathematical model for energy saving in induration of iron ore pellets containing solid fuel. Int. J. Eng. Trans. B: Appl. 16, 265–278.

Hobbs, M.L., Radulovic, P.T., Smoot, L.D., 1993. Combustion and gasification of coals in fixed-beds. Prog. Energy Combust. Sci. 19, 505–586.

Ishida, M., Wen, C.Y., 1971. Comparison of zone-reaction model and unreacted-core shrinking model in solid-gas reactions—I Isothermal analysis. Chem. Eng. Sci. 26, 1043–1048.

Küçükada, K., Thibault, J., Hodouin, D., Paquet, G., Caron, S., 1994. Modeling of a pilot scale iron ore pellet induration furnace. Can. Metall. Q. 33, 1–12.

Levenspiel, O., 1999. Chemical Reaction Engineering, third ed. John Wiley & Sons, Inc., New York.

Majumder, S., Natekar, P.V., Runkana, V., 2009. Virtual indurator: a tool for simulation of induration of wet iron ore pellets on a moving grate. Comput. Chem. Eng. 33, 1141–1152.

Melchiori, T., Canu, P., 2014. Improving the quantitative description of reacting porous solids: critical analysis of the shrinking core model by comparison to the generalized grain model. Ind. Eng. Chem. Res. 53, 8980–8995.

Nouri, S.M.M., Ebrahim, H.A., Jamshidi, E., 2011. Simulation of direct reduction reactor by the grain model. Chem. Eng. J. 166, 704–709.

Patisson, F., François, M.G., Ablitzer, D., 1998. A non-isothermal, non-equimolar transient kinetic model for gas-solid reactions. Chem. Eng. Sci. 53, 697–708.

Sadrnezhaad, S.K., Ferdowsi, A., Payab, H., 2008. Mathematical model for a straight grate iron ore pellet induration process of industrial scale. Comput. Mater. Sci 44, 296–302.

Szekely, J., Evans, J.W., Sohn, H.Y., 1976. Gas-Solid Reactions. Academic Press, New York.
Tan, S., Peng, J., Shi, H., 2016. Modeling and simulation of iron ore pellet drying and induration process with accurate bed void fraction calculation. Drying Technol. 34, 651–664.
Thurlby, J.A., Batterham, R.J., Turner, R.E., 1979. Development and validation of a mathematical model for the moving grate induration of iron ore pellets. Int. J. Miner. Process. 6, 43–64.
Valipour, M.S., Saboohi, Y., 2007. Modeling of multiple noncatalytic gas–solid reactions in a moving bed of porous pellets based on finite volume method. Heat Mass Transfer 43, 881–894.
Wang, J., Peng, J., Balakrishnan, V., Fang, X., 2012. Modeling and simulation of iron ore pellet drying and induration process. In: 24th Chinese Control and Decision Conference (CCDC), Taiyuan, China, pp. 183–187.
Wen, C.Y., Wang, S.C., 1970. Thermal and diffusional effects in noncatalytic solid gas reactions. Ind. Eng. Chem. 62, 30–51.
Wen, C.Y., 1968. Noncatalytic heterogeneous solid fluid reaction models. Ind. Eng. Chem. 60, 34–54.
Yagi, J., Tamura, K., Muchi, I., 1967. Mathematical model of blast furnace supplemented the decomposition rate of lime stone and the molar fractions of CO, CO_2, N_2 and H_2 in top gas. J. Jpn. Inst. Metals Mater. 31, 103–109.
Young, R.W., 1977. Dynamic mathematical model of sintering process. Ironmaking Steelmaking 4, 321–328.